JOURNAL OF MATERIALS SCIENCE 20 (1985) 2087–2092

Influence of nonmetallic inclusions on fatigue crack growth in a structural steel

A. BARBANGELO
Istituto di Meccanica Applicata alle Macchine, Università di Genova, Via all'Opera Pia 15/A, 16145 Genova, Italy

A study of the fatigue behaviour of a hardened and tempered steel, at two inclusion levels, has been carried out according to the linear elastic fracture mechanics criteria. The influence of inclusions on the fatigue crack growth rate has turned out to be a function of the local stress intensity factor range, ΔK_I, at which fracture propagates. At low ΔK_I values, to which are related crack growth rates less than 10^{-5} mm cycle^{-1}, the crack growth rate in the steel with higher inclusion content is lower than in the steel with lower inclusion content. As ΔK_I increases, an inversion in the difference between the two rates occurs. In the "dirtier" steel, the higher ΔK_I, the higher the growth rate than in the other steel. The difference between the two rates becomes nil just below the fast propagation K_{Ic} level. By fractographic analysis, it has been possible to find out how inclusions affect fatigue behaviour.

1. Introduction

In 1971, Thornton [1], in an accurate review of the influence of nonmetallic inclusions on the mechanical properties of steel, pointed out that: "It is possible that nonmetallic inclusions have an explicit effect on the low cycle fatigue properties of steel". Both Pelloux [2] and Heiser [3] made the assumption that the higher fatigue growth rate noticed in an alloy with higher inclusion content might be ascribed to the formation of local fractures at the inclusion–matrix interface.

Subsequently, El-Soudani and Pelloux [4], while studying the fatigue crack growth rate (FCGR) in an aluminium alloy at different inclusion levels, found that inclusions have a beneficial effect on the FCGR in plane strain fracture, and strongly increase the growth rate only in plane stress fracture.

Other studies on steel [5–11] did not show evidence of any correlation between inclusion content and FCGR, even though they also pointed out the influence of inclusions in both the nucleation and growth stages of fatigue fracture. Opposing results were obtained by Raghupathy *et al.* [12], who did not notice any variation in the crack growth rate in a 12% Cr steel, as the sulphide content of the steel changed.

In the present paper, the different effects of inclusions on plane strain fracture in a typical structural steel have been investigated. For this purpose, the fatigue behaviour of two steels with about the same chemical composition and microstructure has been examined using the method of linear elastic fracture mechanics; such steels contained inclusions of the same types and sizes but at different inclusion levels. Moreover, an accurate fractographic analysis has been carried out in order to identify the effects of inclusions under the various crack propagation conditions.

2. Experimental procedures

2.1. Materials

Two 30 NiCrMo 12–V steels were chosen, one of commercial purity (steel 1) and the other (obtained by particularly accurate steelmaking) with a low inclusion content (steel 2). Their chemical compositions are given in Table I.

From rods 290 mm diameter, normalized at

0022–2461/85 $03.00 + .12

TABLE I Chemical composition of the steels considered (wt %)

	C	Ni	Cr	Mo	V	Mn	Si	S	P	As	Sn	Al
Steel 1	0.30	3.14	1.24	0.53	0.17	0.63	0.41	0.008	0.008	0.014	0.007	0.005
Steel 2	0.33	3.50	1.58	0.50	0.11	0.45	0.45	0.010	0.004	0.010	0.014	0.011

880° C, 30 mm x 30 mm x 180 mm bars were obtained, which were hardened by oil quenching from 840° C and tempered 1.5 h at 640° C. The two hardened and tempered steels exhibited the mechanical and metallurgical characteristics given in Table II.

As far as their inclusion contents are concerned, the dominant inclusions in the two steels were spheroidal oxides, with the presence of sulphides and alumina. The inclusion sizes were similar in the two cases, with the 0.5 size [14] prevailing.

2.2. Test apparatus and techniques

To perform fatigue tests, from the hardened and tempered rods, standard compact-type (CT) specimens for mode-I deformation (tension stress perpendicular to crack surfaces), with geometry according to the BS specification [15], were obtained. Details of the specimen geometry are shown in Fig. 1. Particular care was exercised in machining the notch and in precracking the specimens. The notch was made by electrical-discharge machining, and the final maximum stress intensity factor, K_{Imax}, during precracking did not exceed the initial K_{Imax} for which test data were obtained. Six specimens for each type of steel were subjected to fatigue in air, using tension test machines of the Mayes Unisteel type, modified in order to suit them to dynamic tests.

TABLE II Mechanical and metallurgical properties of the steels considered

Property		steel 1	steel 2
Tensile strength (MPa)		1173	1087
0.2% yield strength, σ_y (MPa)		712	837
Elongation (%), $L_o = d_o$		14.6	14.8
Impact toughness Charpy-U longitudinal (J cm^{-2})		68	109
Impact toughness Charpy-U transverse (J cm^{-2})		56	82
Rockwell C hardness		33	31
Microstructure		tempered martensite	tempered martensite
Austenitic grain size 13	grade	6/7	6/7
	longitudinal	22.5	14.5
Nonmetallic micro-	transverse	18.0	13.5
inclusion content [14]	total rating numbers	40.5	28.0

By such an apparatus it is possible to impose, and keep unchanged in the course of a test, the maximum load value applied. During the test, the value of the minimum load actually applied increases, and then the typical ratio, R, between the minimum and the maximum loads applied increases.

The fatigue tests were performed at a load application frequency of 2 Hz, with maximum load values equal to 3220 N, and with R values ranging from 0.25 to 0.56. The crack length was measured with a metrological microscope at set intervals of the number of the load application cycles, according to the BS specification [15].

During the tests, the value of the minimum load actually applied to each specimen was recorded as the crack length changed. The results obtained from the fatigue tests, namely from the crack length measurements as the number of fatigue cycles varied, were processed in order to determine the crack growth rate, $(\mathrm{d}a/\mathrm{d}N)$, as a function of the stress intensity factor range in mode I deformation, (ΔK_{I}).

The crack growth rate is taken as the slope of the tangent to the crack length against number-of-cycles curves. The stress intensity factor for the opening mode was calculated through the following relationship [15]:

$$\Delta K_{\mathrm{I}} = \frac{\Delta P}{BW^{1/2}}\left[29.6\left(\frac{a}{W}\right)^{1/2} - 185.5\left(\frac{a}{W}\right)^{3/2} + 655.7\left(\frac{a}{W}\right)^{5/2} - 1017.0\left(\frac{a}{W}\right)^{7/2} + 638.9\left(\frac{a}{W}\right)^{9/2}\right]$$

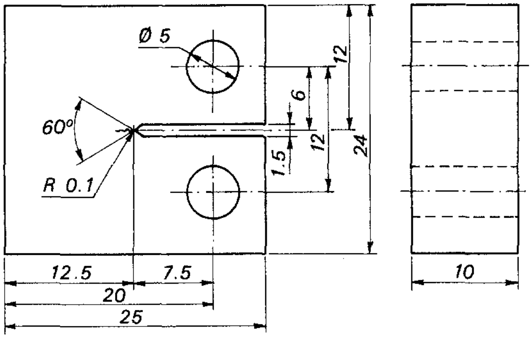

Figure 1 Test piece. Dimensions in mm.

were a is the crack length in metres; ΔP is the algebraic difference, in newtons, between the maximum and minimum loads in a fatigue cycle; B is the test-piece thickness in metres; and W is the test-piece width in metres.

The da/dN against ΔK_I curves allow one to determine, by vertical asymptote, the critical value of the stress intensity factor range for unstable crack growth, ΔK_{Ic}. The plane strain fracture toughness, K_{Ic}, which is the K_{Imax} corresponding to ΔK_{Ic}, is calculated as

$$K_{Ic} = \frac{\Delta K_{Ic}}{1-R}$$

The fracture surfaces of the specimens subjected to the fatigue tests were examined with a scanning electron microscope (SEM) and an energy dispersion microprobe. All the SEM fractography observations were done with the fracture surface at 0° tilt in order to have a true projected area.

By using the SEM nonius, it was possible to measure the distance of the area under examination from the crack tip, and then to identify the local crack propagation conditions.

3. Results

3.1. Fatigue tests

The processing of the data obtained from the fatigue tests allowed the values of the crack growth rates in the two steels to be deduced as a function of the stress intensity factor ranges. Six tests were run for each steel and only one set of results are plotted (curves (a) and (b) in Fig. 2) as the growth rates were within ± 5% of each other.

For ΔK_I values less than 13 MPa m$^{1/2}$, to which crack growth rates less than 10^{-5} mm cycle^{-1} are related, the crack propagation rate in the steel with higher inclusion content is lower than in the other steel. As ΔK_I increases, the behaviours of the two steels are reversed.

The crack propagation rate in the steel with higher inclusion content becomes higher than in the other steel. Moreover, the difference between the two rates keeps on increasing with increasing ΔK_I. As propagation approaches instability conditions, the difference between the two rates suddenly decreases, until it becomes null. The difference between the FCGRs in the two steels is shown in Fig. 3.

The critical stress intensity factor range, ΔK_{Ic}, turns out to be the same in the two steels and equal to 28 MPa m$^{1/2}$. This value leads to a frac-

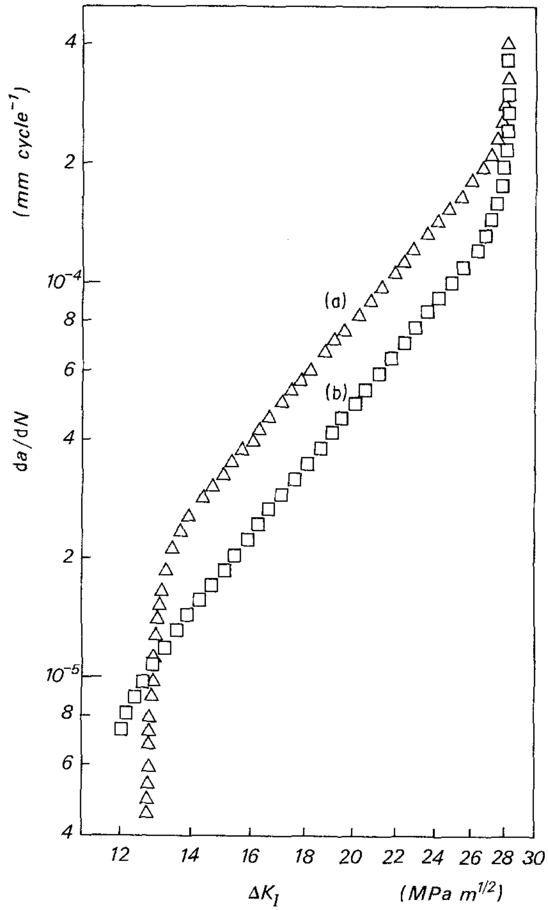

Figure 2 Fatigue crack growth rate, da/dN, as a function of stress intensity factor range, ΔK_I: (a) steel 1; (b) steel 2.

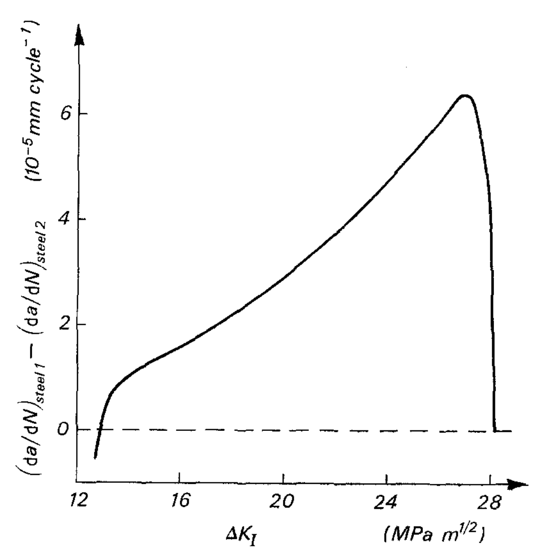

Figure 3 Difference between the fatigue crack growth rates in the two steels considered, as a function of stress intensity factor range.

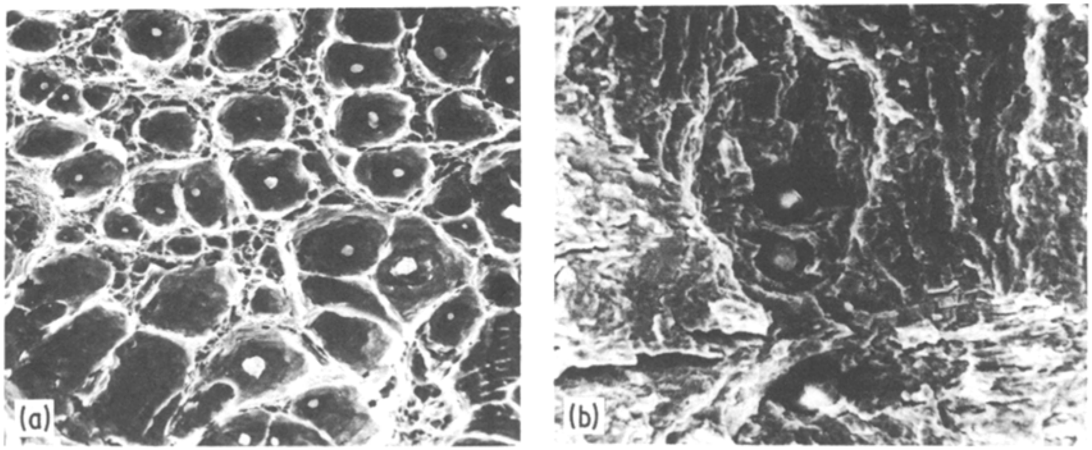

Figure 4 Voids coalescence: (a) in the region of final, fast fracture (× 1400); (b) sporadical occurrence in the region of subcritical fatigue crack propagation (× 750).

ture toughness $K_{Ic} = 64\,\mathrm{MPa\,m^{1/2}}$. However, it is worth noting that for ΔK_I values greater than $26\,\mathrm{MPa\,m^{1/2}}$, the relationship $B > 2.5\ (K_{Imax}/\sigma_y)^2$, suggested by the BS specification [15], it is no longer valid. Nevertheless, the above data maintain their validity if they are regarded not as absolute values but as a comparison between the behaviours of the two steels.

3.2. Fractographic analysis

A fractographic analysis of the fracture surfaces evidenced the role played by inclusions in fatigue fracture propagation. In the presence of inclusions, fatigue causes inclusion–matrix decohesions; the shape and size of such voids depend both on the type and size of the inclusions around which voids nucleate, and on the stress intensity conditions of fracture propagation.

Moreover, it can be noticed that, unlike what has been found in the case of final, fast fracture, in fatigue fracture the formation of voids occurs only around inclusions on the fracture plane, or those which are very near to it, and coalescence of voids hardly occurs, that is, only when the inclusions that generate them are sufficiently close to each other (Fig. 4).

The shape and size of inclusion voids can vary considerably with varying fracture propagation conditions. Fig. 5 presents, in a schematic way, the evolution of inclusion decohesions as the ΔK_I value, at which fracture formed, increases.

At low ΔK_I values, near the threshold stress intensity factor range, rather small voids form around inclusions. As ΔK_I increases, such voids become larger and larger, elongating in the direction of crack propagation. Then their shape becomes round again and their size gets smaller as the propagation rate approaches critical values. The latter voids appear to be similar to those generated by inclusions in final, fast fracture propagation but no coalescence occurs among them, and they remain in isolation on the fatigue fracture surface. The fractographs in Fig. 6 represent the typical variation in the morphology of inclusion voids as ΔK_I increases.

4. Discussion

A comparison between the (da/dN) against ΔK_I curves and the fractographic observations has

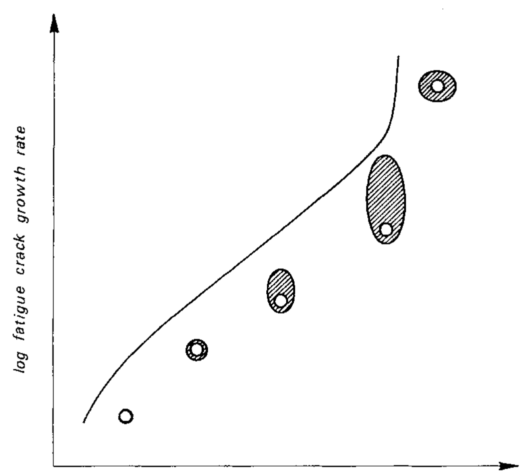

Figure 5 Schematic presentation of inclusional cavity shapes and sizes as a function of stress intensity factor range.

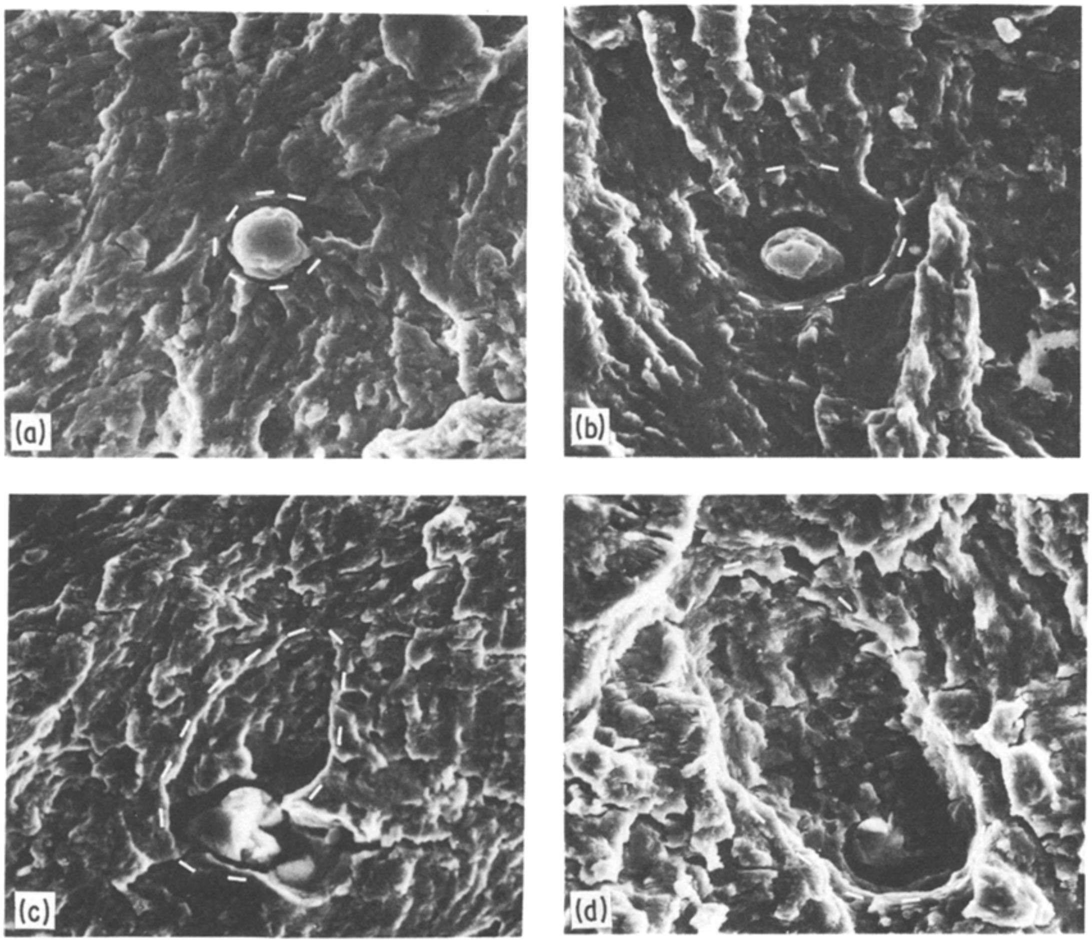

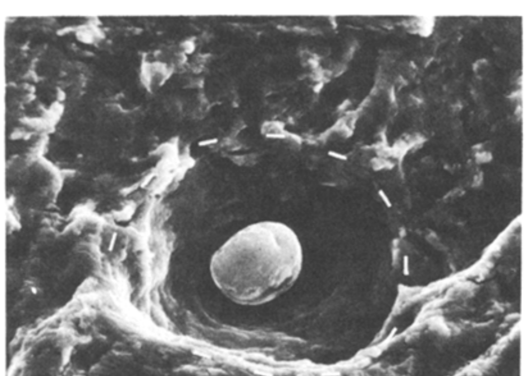

Figure 6 Fractographs of cavities (outlined by a dashed line) formed around inclusions at different local stress intensity factor range values: (a) $\Delta K_{\mathrm{I}} = 12$ MPa m$^{1/2}$ ($\times$ 2200); (b) $\Delta K_{\mathrm{I}} = 14$ MPa m$^{1/2}$ ($\times$ 2200); (c) $\Delta K_{\mathrm{I}} = 17.5$ MPa m$^{1/2}$ ($\times$ 1500); (d) $\Delta K_{\mathrm{I}} = 24$ MPa m$^{1/2}$ ($\times$ 2200); (e) $\Delta K_{\mathrm{I}} = 27.5$ MPa m$^{1/2}$ ($\times$ 3500).

allowed us to state that the crack growth rate depends directly on the surface extent of inclusions–matrix decohesions, and then on the number and extent of such voids. Inclusion–matrix voids have a twofold effect on the crack growth rate: on one hand, the decohesion mechanism replaces, in part, the propagation mechanism in the matrix; on the other hand, the presence of voids causes an increase in the matrix FCGR, in that the applied load is distributed on a smaller real surface.

The presence of inclusions has a more detrimental effect on the fatigue properties whenever propagation conditions are such that larger inclusion–matrix decohesions occur. The two steels under investigation contain inclusions which are similar in shape and size so that their different fatigue crack growth rates only depend on the different number of inclusions and on the extent of the voids generated by these inclusions. In particular, the difference between the propagation rates, at the same ΔK_I, is to be related to the number of inclusion voids, whereas the behaviour of the difference in crack growth rates, as ΔK_I increases, is due both to the different extent of the voids that form under the different local propagation conditions, and to the different influence exerted by a smaller load application real surface as ΔK_I increases.

The analysis of the variations in the size of voids caused by inclusions under varying propagation conditions (see Fig. 5) suggests that inclusions cause the greatest damage during subcritical crack propagation, at high ΔK_I values, whereas their influence is negligible in critical crack propagation and near threshold. The difference in the crack growth rates in the two steels with different inclusion content (Fig. 3) confirms this conclusion concerning both subcritical and critical crack propagation.

Near threshold, at low ΔK_I values, for FCGR values less than 10^{-5} mm cycle^{-1}, inclusions have a beneficial effect on fatigue properties. At very low FCGR values, this effect may be due, as suggested by McEvily [16], to a crack blunting or to a distribution of the crack tip opening displacements over different crack levels and different crack modes, as shown by El Soudani and Pelloux [4]. Both hypotheses are consistent with the size of the voids observed. In fact, both beneficial mechanisms can prevail over damage only if voids are small, which can occur only at very low ΔK_I values.

The different effects of inclusions in the different propagation regions, as suggested by fractographic analysis, have been assessed in the case of a structural steel, though they might be regarded as general detrimental effects of inclusions on the fatigue properties of steel.

Acknowledgement

The author gratefully acknowledges the help of the Tassara Breno S.p.A. Steelworks, for supplying the materials.

References

1. P. A. THORNTON, *J. Mater. Sci.* **6** (1971) 347.
2. R. M. N. PELLOUX, *Trans. ASM* 57 (1964) 511.
3. F. A. HEISER, "Anisotropy of Fatigue Crack Propagation in Hot Rolled Steel Plate", Watervliet Arsenal Report WVT-6931, (1969).
4. S. M. EL-SOUDANI and R. M. PELLOUX, *Met. Trans.* **4** (1973) 519.
5. I. P. VOLCHOK, S. E. KOVCHIK, V. V. PANASYUK and U. A. SHULTE, *FKH MM (Sov. Mater. Sci.)* **3** (1967) 439.
6. F. B. STULEN, H. N. CUMMINGS and W. C. SCHULTE, Proceedings of the International Conference on Fatigue of Metals, (Institute of Mechanical Engineers, London, 1956) p. 439.
7. H. N. CUMMINGS, F. B. STULEN and W. C. SCHULTE, *Trans. ASM* **49** (1957) 482.
8. J. T. RANSON, *Trans. ASTM* **46** (1954) 1254.
9. H. N. CUMMINGS, F. B. STULEN and W. C. SCHULTE, *Proc. ASTM* **58** (1958) 505.
10. M. ATKINSON, *J. Iron Steel Inst.* **195** (1960) 64.
11. E. SCHMIDTMANN, W. ECKEL and G. WELLNITZ, *Arch. Eisenhüttenwesen* **53** (1982) 157.
12. V. P. RAGHUPATHY, V. SRINIVASAN, K. KRISHNAN and M. N. CHANDRASEKHARAIAH, *J. Mater. Sci.* **17** (1982) 2112.
13. ASTM E 112 (American Society for Testing and Materials, Philadelphia, 1963).
14. ASTM E 45–76 Tab. III, Met. D (American Society for Testing and Materials, Philadelphia, 1976).
15. British Standard DD3, "Methods for Plane Strain Fracture Toughness (K_{Ic}) Testing" (1971).
16. A. J. McEVILY, NASA, TD D328 (1962).

Received 16 April
and accepted 31 July 1984